01 Jan 1992

A Complete Model Characterization of Brushless DC Motors

N. Hemati

Ming-Chuan Leu
Missouri University of Science and Technology, mleu@mst.edu

Recommended Citation

A Complete Model Characterization of Brushless dc Motors

Neyram Hemati, *Member, IEEE*, and Ming C. Leu, *Member, IEEE*

Abstract—This paper addresses the modeling problem associated with brushless dc motors (BLDCM's) with nonuniform air gaps that operate in a range where magnetic saturation may exist. The mathematical model includes the effects of reluctance variations as well as magnetic saturation to guarantee proper modeling of the system. An experimental procedure is developed and implemented in a laboratory environment to identify the electromagnetic characteristics of a BLDCM in the presence of magnetic saturation. It is demonstrated that the modeling problem associated with this class of BLDCM can be formulated in terms of mathematically modeling a set of multidimensional surfaces corresponding to the electromagnetic torque function and the flux linkages associated with the motor phase windings. The accuracy of the mathematical model constructed by the developed method is checked against experimental measurements.

I. INTRODUCTION

IN RECENT YEARS, brushless motors have become a viable choice for motion control applications such as robotics, aerospace, numerically controlled machine tools, electric propulsion, and many more [1], [3], [15], [16], [21]. The increasing interest has been a consequence of the advantages of brushless motors compared with the conventional dc motors. These advantages are mainly the result of the elimination of the physical contact between the mechanical brushes and commutators. Among the numerous types of brushless motors, the brushless dc motor (BLDCM) has emerged as the one with the highest potential in high-performance applications [1], [3], [15], [16]. In particular, BLDCM has been an attractive choice for direct-drive applications [1], [15], where large torques are required for high acceleration and deceleration rates. For such high-performance applications, the mathematical model of BLDCM must include the effects of reluctance variations and, most importantly, the magnetic saturation whose existence is inevitable when large torques are generated.

In the past, due to the complexity involved, the tasks of modeling, analysis, and control of BLDCM have been based on a number of simplifying assumptions, namely, the air gap has been assumed to be uniform and/or the magnetic struc-

ture has been assumed to be linear [1], [3], [9], [11], [14], [15], [17], [18], [20]. Persson and Buric [17] considered the mathematical modeling of a BLDCM with an arbitrary number of stator phase windings and permanent magnet pole pairs. Their work, however, was solely based on the assumption of having uniform air gaps and the absence of magnetic saturation. In [3], Demerdash *et al.* presented digital simulation techniques to demonstrate the feasibility of using BLDCM's for electric propulsion applications, where they considered BLDCM's with uniform air gaps and linear magnetic structures. The problem of optimal phase advancing to enhance the torque generation of a BLDCM has been addressed by numerous authors, e.g., [11], [14], [20], whose results are based on the assumption that the reluctance variations are negligible. Krause *et al.* [11] and Jahns [9] have used mathematical models that include the effect of reluctance variations to present some analytical results without addressing the saturation nonlinearity effects.

Another class of brushless motors that has attracted wide attention in the motion control industry is the switched reluctance motor (SRM). Similar to the BLDCM, the SRM has also been the subject of numerous research projects and publications [2], [7], [8], [13], [19]. However, the SRM constitutes a fundamentally different dynamical system than the BLDCM. The difference lies in the fact that the phase windings of the SRM are decoupled, whereas in a BLDCM, the coupling is significant. In other words, although it is common to neglect the effect of mutual inductances associated with the phase windings in a SRM, this is not a valid assumption in a BLDCM. The coupling among the phase windings introduces a significant problem, which is resolved in Section IV.

This paper presents a method of constructing accurate BLDCM models where both magnetic saturation and reluctance variation effects have been accounted for. It is demonstrated that an accurate description of the characteristics of BLDCM may be obtained by modeling the torque function and the flux linkages associated with the stator phase windings as 4-D surfaces. However, for the mathematical model to be computationally feasible in real-time motion control applications, a method that is used to reduce the complexity of the model without sacrificing its accuracy is presented. If the mathematical model is excessively complex, one will have to resort to incorporating look-up tables in real-time motion control applications [7]. To keep the complexity of the mathematical model within feasible limits, through physical reasoning, it is demonstrated that the modeling problem may be reduced to that of identifying a set of 2-D surfaces.

N. Hemati is with the Department of Mechanical Engineering and Mechanics, Drexel University, Philadelphia, PA 19104.
M. C. Leu is with the Department of Mechanical and Industrial Engineering, New Jersey Institute of Technology, Newark, NJ 07102.

Based on this, a practical method for constructing accurate models of a BLDCM is outlined and shown to be effectively implementable in a typical laboratory environment.

The paper is organized as follows. In Section II, the fundamental electromechanical characteristics of the BLDCM are formulated in terms of a set of mathematical relationships. Section III sets forth some analytical results that are used to demonstrate the importance of including the effect of reluctance variations in the BLDCM model. Section IV deals with the problems associated with the modeling of the saturation nonlinearity for a BLDCM. Section V presents an experimental procedure used in identifying the mathematical model of a BLDCM. The results corresponding to the set of experiments that have verified the validity of the methods described in the earlier sections are presented in Section VI. Finally, some concluding remarks are made in Section VII.

II. BLDCM WITHOUT MAGNETIC SATURATION

A BLDCM consists of a permanent magnet rotor, a position sensor mounted on the rotor, and a means to provide signals to the stator winding (see Fig. 1). In the absence of magnetic saturation, the governing differential equations describing the dynamic behavior of BLDCM may be written as

$$\underline{V}(t) = \underline{R}\underline{I}(t) + \frac{d\underline{\Lambda}(\underline{I}, \theta)}{dt} \tag{1}$$

where θ is the position variable $\underline{V} = [v_1, v_2, v_3]^T$, and $\underline{I} = [i_1, i_2, i_3]^T$ are the phase voltage input and current vectors, respectively. $\underline{R}$ is the resistance matrix, and the flux linkage vector is defined by

$$\underline{\Lambda}(\underline{I}, \theta) = \underline{L}(\theta)\underline{I} + \underline{\Lambda}_m(\theta) \tag{2}$$

where the inductance matrix $\underline{L}(\theta)$ is a 3-by-3 symmetric matrix whose diagonal elements are the self inductances, and its off-diagonal elements are the mutual inductances of the windings and are defined by

$$L_{kk} = L_a - L_g \cos\left(2n\theta + \frac{2(k-1)\pi}{3}\right)$$

$$\text{for } k = 1, 2, 3 \tag{3}$$

$$L_{12} = L_{21} = -\frac{L_a}{2} - L_g \cos\left(2n\theta - \frac{2\pi}{3}\right) \tag{4}$$

$$L_{13} = L_{31} = -\frac{L_a}{2} - L_g \cos\left(2n\theta - \frac{4\pi}{3}\right) \tag{5}$$

$$L_{23} = L_{32} = -\frac{L_a}{2} - L_g \cos\left(2n\theta\right). \tag{6}$$

L_a is the nominal (average) value of the winding inductance, L_g represents the amplitude of variation in the inductance due to the nonuniformity of the air gap, and n is the number of permanent magnet pole pairs. The elements of the permanent magnet flux linkage vector, $\underline{\Lambda}_m(\theta)$, i.e., λ_{mk}, $k = 1, 2, 3$, represent the flux linkages associated with the permanent magnet and phase k. For sinusoidally distributed stator windings, λ_{mk} may be written as

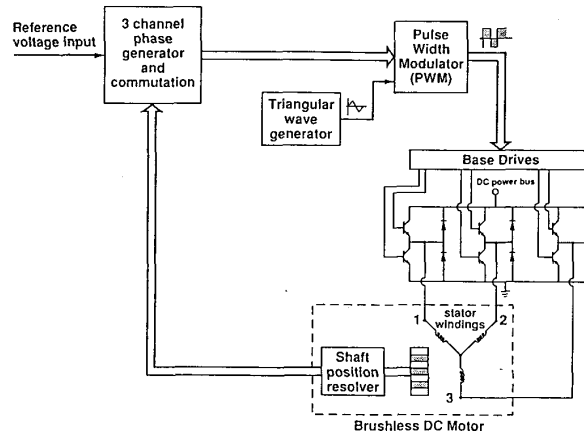$$\lambda_{mk} = K_e \sin\left(n\theta - \frac{2(k-1)\pi}{3}\right) \quad k = 1, 2, 3 \tag{7}$$

Fig. 1. Typical brushless dc motor and its commutation.

where K_e is the electromotive force, i.e, the back EMF, constant. The expression for the torque generated by the motor as a function of phase currents and rotor displacement is

$$T(\underline{I}, \theta) = nL_g \left\{ 2\left(\sin\left(2n\theta - \frac{2\pi}{3}\right)i_1 i_2\right.\right.$$

$$+ \sin\left(2n\theta + \frac{2\pi}{3}\right)i_1 i_3 + \sin\left(2n\theta\right)i_2 i_3\right)$$

$$+ \sum_{k=1}^{3} i_k^2 \cos\left(2n\theta + \frac{2(k-1)\pi}{3}\right)\right\}$$

$$+ nK_e \sum_{k=1}^{3} i_k \cos\left(n\theta - \frac{2(k-1)\pi}{3}\right). \tag{8}$$

Equation (1) represents a system of differential equations with time varying (periodic) coefficients. It is known [4], [10], [22] that for sinusoidally distributed windings, a Floquet transformation, which is frequently referred to as the Park's transformation, may be used to transform the above equations to a system of differential equations with constant coefficients, represented in a coordinate frame attached to the rotor. This orthogonal transformation can be expressed in the matrix form as

$$\begin{bmatrix} \sigma_q \\ \sigma_d \\ \sigma_0 \end{bmatrix} = \sqrt{\frac{2}{3}}$$

$$\cdot \begin{bmatrix} \cos\left(n\theta\right) & \cos\left(n\theta - \frac{2\pi}{3}\right) & \cos\left(n\theta + \frac{2\pi}{3}\right) \\ \sin\left(n\theta\right) & \sin\left(n\theta - \frac{2\pi}{3}\right) & \sin\left(n\theta + \frac{2\pi}{3}\right) \\ \frac{\sqrt{2}}{2} & \frac{\sqrt{2}}{2} & \frac{\sqrt{2}}{2} \end{bmatrix}$$

$$\cdot \begin{bmatrix} \sigma_1 \\ \sigma_2 \\ \sigma_3 \end{bmatrix}. \tag{9}$$

The subscripts 1, 2, and 3 correspond to the stator windings, whereas the subscripts q, d, and 0 represent some fictitious windings attached to the rotor. The variables σ_1, σ_2, σ_3, σ_q, σ_d, and σ_0 may represent voltages, currents, or flux linkages. For convenience, we shall use a slightly different form of this transformation by replacing the last row in the transformation matrix by a row of $\frac{1}{2}$'s and replacing the scalar constant $\sqrt{\frac{2}{3}}$ by $\frac{2}{3}$. As a result, the transformed set of equations describing the behavior of BLDCM in the rotating frame become

$$v_q(t) = Ri_q(t) + n\lambda_d(t)\frac{d\theta(t)}{dt} + \frac{d\lambda_q(t)}{dt} \quad (10)$$

$$v_d(t) = Ri_d(t) + \frac{d\lambda_d(t)}{dt} - n\lambda_q(t)\frac{d\theta(t)}{dt} \quad (11)$$

where

$$\lambda_q(t) = L_q i_q(t) \quad (12)$$

$$\lambda_d(t) = L_d i_d(t) + K_e \quad (13)$$

and

$$L_q = \left(\frac{3}{2}\right)(L_a - L_g) \quad (14)$$

$$L_d = \left(\frac{3}{2}\right)(L_a + L_g). \quad (15)$$

The torque expression after the application of the transformation becomes

$$T(i_q, i_d) = \left(\frac{3n}{2}\right)\{\lambda_d(t)i_q(t) + \lambda_q(t)i_d(t)\}. \quad (16)$$

In the following section, the description of a BLDCM in the rotating frame is used to show some analytical results, which compare the torque-speed characteristics of a BLDCM with uniform and nonuniform air gaps.

III. Torque-Speed Characteristics of a BLDCM

In the previous works related to the modeling of a BLDCM, it has been common to neglect the reluctance variation terms [1], [3], [14], [15], [17], [20]. In this section, we will demonstrate that this may have adverse affects on the analytical results that one obtains. Fig. 2 shows the torque-speed characteristics of the BLDCM whose specifications have been tabulated in Table I. The figure consists of the torque-speed ($T - \omega$) curves of the BLDCM for the case when the reluctance variations have been accounted for and when they have been neglected. As depicted in the figure, the reluctance variations affect the torque output in a favorable way. Accordingly, some researchers, e.g., [9], have used this desirable factor to design permanent magnet motors with better torque producing capabilities by introducing significant saliency in the motor. Here, we will demonstrate the adverse effect of neglecting the reluctance variations on the motor characteristics by considering the optimal phase advancing scheme [11], [14], [20].
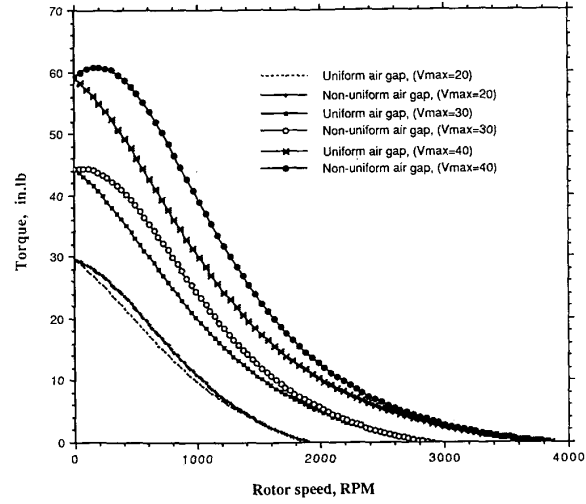

Fig. 2.   Torque-speed characteristics of the BLDCM based on the uniform and the nonuniform air-gap models.

TABLE I
NUMERICAL VALUES FOR THE PARAMETERS OF THE BLDCM (MOOG 303-003) IN THE LINEAR RANGE OF OPERATION

PARAMETER	Numerical Values	Units
n	4	—
R	0.9	Ohms
K_e	0.02502	Volts/Radians/Seconds
L_a	0.95	milli-Henries
L_g	0.2	milli-Henries

For the constant speed operation of a BLDCM, the voltage inputs across the stator phase windings may be written as

$$v_k = V_{\max}\cos\left(n\theta - \frac{2(k-1)\pi}{3} - \phi\right) \quad k = 1, 2, 3 \quad (17)$$

where ϕ is a phase shift that may be varied to alter the torque-speed characteristics of the motor. When the reluctance variations are neglected, the torque generated as a function of the phase shift ϕ may be written as

$$T(\phi) = \left\{\frac{3nK_e R}{2\left[R^2 + (nL_q\omega)^2\right]}\right\}$$

$$\cdot\left\{V_{\max}\left[\cos(\phi) - \left(\frac{nL_q\omega}{R}\right)\sin(\phi)\right] - nK_e\omega\right\}. \quad (18)$$

The torque function (18) has a maximum at

$$\phi = -\tan^{-1}\left(\frac{nL_s\omega}{R}\right) \quad \text{where } \frac{-\pi}{2} < \phi < 0 \quad (19)$$

which is referred to as the "optimal phase advance" [14], [20]. Fig. 3 shows the effect of the optimal phase advance on the torque-speed characteristics of the BLDCM, assuming that the air gap is uniform. However, if this "optimal" phase advance is incorporated in altering the characteristics of the actual motor, i.e., the nonuniform air-gap motor, then the
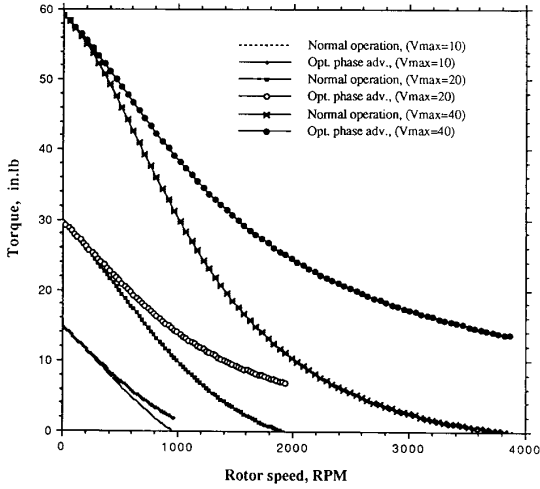
Fig. 3. Torque-speed characteristics of the uniform air-gap BLDCM with and without the optimal phase advance in the voltages across the phase windings.
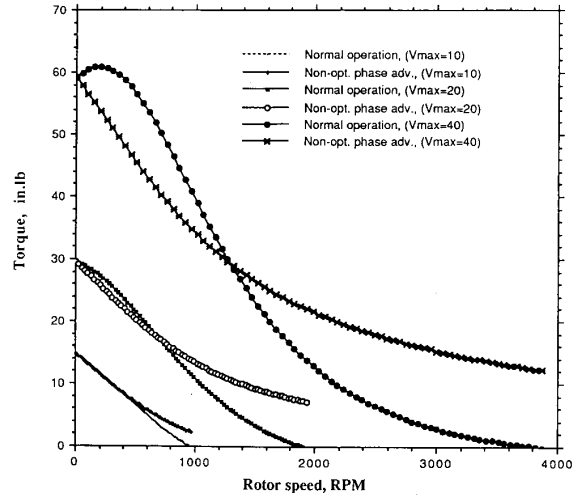

Fig. 4. Torque-speed characteristics of the nonuniform air-gap BLDCM for the normal operation and when the phase advance is computed based on the uniform air-gap model.

enhancement in the $T - \omega$ curves will only exist at high operating speeds; see Fig. 4. As depicted in this figure, the incorporation of the "optimal" phase advance computed based on a uniform air-gap model actually degrades the $T - \omega$ characteristics at lower operating speeds. This degradation would be even more pronounced if the BLDCM were to have more significant variations in its air-gap reluctance; see Fig. 5. These suggest that in order to enhance the $T - \omega$ characteristics of the nonuniform air-gap BLDCM, the optimal phase advance must be computed based on the model that includes the effect of reluctance variations.

When the reluctance variations have been taken into account, and for a constant rotor speed, the torque equation as a function of ϕ may be written as

$$T(\phi) = \left(\frac{3n}{2}\right)$$

$$\cdot \left[K_e + \left(L_d - L_q\right)\frac{n\omega L_q i_q + V_{max}\sin\left(\phi\right)}{R}\right] i_q \quad (20)$$

where

$$i_q = \frac{V_{max}\left[\cos\left(\phi\right) - \frac{n\omega L_d}{R}\sin\left(\phi\right)\right] - nK_e\omega}{R\left(1 + \frac{n^2\omega^2 L_d L_q}{R^2}\right)}. \quad (21)$$

To determine the value of ϕ that would maximize $T(\phi)$, it is necessary to use numerical techniques. Fig. 6 shows the torque-speed characteristics of the BLDCM for both the normal operation, i.e., $\phi = 0$, and when the optimal phase advance, which is computed by maximizing $T(\phi)$ in (20), has been incorporated.

IV. BLDCM WITH MAGNETIC SATURATION

In this section, we will consider the presence of magnetic saturation. A procedure will be outlined and then imple-
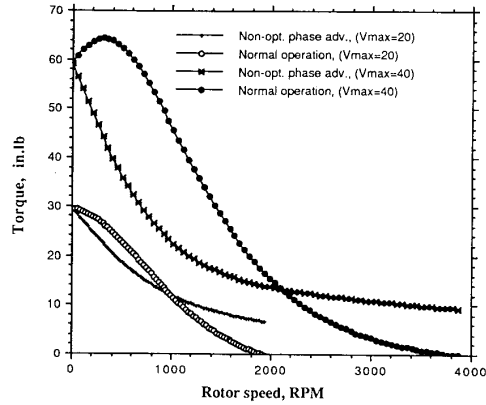

Fig. 5. Torque-speed characteristics of a nonuniform air-gap BLDCM with twice as much saliency for the normal operation and when the phase advance has been computed based on the uniform air-gap model.
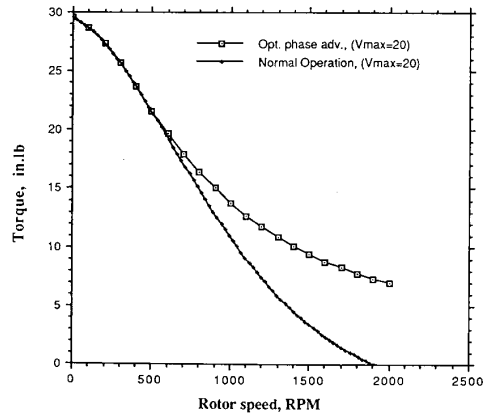

Fig. 6. Torque-speed characteristics of the nonuniform air-gap BLDCM with and without the optimal phase advance in the voltage inputs.

mented for construction of accurate BLDCM mathematical models when magnetic saturation and reluctance variations are present. In Section II, the flux linkages were in terms of constant inductance parameters; see (2)–(6). However, when magnetic saturation is present, the flux linkages are no longer linear functions of the phase currents, and one can only state that

$$\lambda_k = \lambda_k(i_1, i_2, i_3, \theta) \qquad k = 1, 2, 3. \qquad (22)$$

In other words, the flux linkages define a set of 4-D surfaces in a 5-D space. It is possible to experimentally obtain these flux linkage surfaces. Recalling (1) and for a fixed value of $\theta = \theta^*$, one can write

$$\lambda_k(i_1, i_2, i_3, \theta^*) = \int_0^t \left[v_k(\tau) - Ri_k(\tau) \right] d\tau. \qquad (23)$$

This may be used in constructing the flux linkage surfaces as follows. By appropriately varying phase voltages v_k or currents i_k and sampling their values, the integral in (23) can be computed. The corresponding values of the integral will then define a set of discrete data points that lie on the flux linkage surfaces. Using numerical techniques, one can then compute approximate mathematical representations for these surfaces. Once a set of mathematical representations for the flux linkages have been obtained, one can then derive the torque expression by first constructing the coenergy function

$$
\begin{aligned}
W_c(i_1, i_2, i_3, \theta) = &\int_0^{i_1} \lambda_1(\theta, \xi, 0, 0) \, d\xi \\
&+ \int_0^{i_2} \lambda_2(\theta, i_1, \eta, 0) \, d\eta \\
&+ \int_0^{i_3} \lambda_3(\theta, i_1, i_2, \zeta) \, d\zeta \quad (24)
\end{aligned}
$$

and then

$$T(i_1, i_2, i_3, \theta) = \frac{\partial W_c(i_1, i_2, i_3, \theta)}{\partial \theta} \qquad (25)$$

where in (24), ξ, η, and ζ are dummy variables of integration.

Our main purpose for constructing an accurate mathematical model for a BLDCM has been to be able to incorporate it in control applications. However, the modeling procedure stated above will result in complex mathematical relationships, which are computationally unattractive for real-time control purposes. Furthermore, as illustrated in (25), the torque expression depends explicitly on rotor displacement that leads to the need for constructing explicit commutation strategies. This could make the real-time control of a BLDCM with magnetic saturation infeasible. In the following subsection, a different approach that eliminates the need for such a complex model formulation, is presented.

A. BLDCM Model in Rotating Frame

In the absence of magnetic saturation, Park's transformation was used in Section II to obtain a simplified formulation for a BLDCM in a rotating frame attached to the rotor. This eliminated the dependence of the inductance parameters and the torque expression on the rotor displacement. However, when magnetic saturation is present, Park's transformation

does not apply if the flux linkages are expressed by nonlinear functions. To render this transformation valid, we formulate the behavior of the BLDCM with magnetic saturation by a piecewise linear model. In other words, the flux linkages are modeled by piecewise linear functions of the phase currents. This in turn allows us to apply the Park's transformation to obtain a simplified description of a BLDCM with magnetic saturation. The parameters defining the flux linkages, i.e., inductances and electromotive force constant, now become piecewise constant functions of the phase currents. The BLDCM with magnetic saturation is represented in the rotating frame by a set of equations similar to (10)–(15), except that now, the inductance parameters L_a and L_g and the electromotive force constant K_e are piecewise constant functions of the phase currents. This in turn defines a piecewise linear model for the flux linkages λ_q and λ_d.

Consequently, the characteristics of the saturated BLDCM are described by three piecewise constant functions of current: $L_a(i)$, $L_g(i)$, and $K_e(i)$. Since the flux linkages corresponding to the individual phase windings are all functions of these three parameters, the experimental identification process may be performed for each phase winding independently of the rest. Considering one phase winding at a time, we have

$$
\begin{aligned}
\lambda_k(i_k, i_j = 0, i_m = 0, \theta) &= \lambda_k(i_k, \theta) \\
&j, k, m = 1, 2, 3, \; j \neq k \neq m. \quad (26)
\end{aligned}
$$

The flux linkage λ_k now represents a 2-D surface rather than a 4-D surface. As was done in (23), we can now write

$$\lambda_k(i_k, \theta) = \int_0^t \left[v_k(\tau) - Ri_k(\tau) \right] d\tau \qquad k = 1, 2, 3. \qquad (27)$$

The surfaces representing the flux linkages may then be constructed by sampling the voltage v_k and the current i_k and computing the integral in (27). Once a sufficient number of data points on the flux linkage surfaces have been collected, we can obtain a mathematical representation for each of these surfaces by using numerical optimization techniques. This will be discussed in Section VI.

Usually, in a BLDCM, the resistance R is much larger in value than the inductances L_a and L_g. Consequently, for the inductance voltage drop $L(di_k / dt)$ to be in the same order of magnitude as the resistance voltage drop Ri_k, the time rate of change of current must be very large. In performing experiments, this large current rate is needed if the voltage information is to be used to determine an accurate description of the flux linkages. However, this requires a power supply capable of providing currents at high frequencies and in turn results in the need for expensive instrumentation. To remedy this problem, we use an alternative approach for performing experiments and data collection as presented below.

V. Experimental Determination of BLDCM Model

The experimental procedure outlined in Section IV can be implemented satisfactorily only if appropriate power supplies and instrumentation are available. To remedy these limita-

tions, we have based our experimental method on the following alternative approach. The method incorporates torque and current measurements for the rotor locked at various rotor displacements to construct the coenergy function associated with the BLDCM. The coenergy function is expressed as

$$W_c(i, \theta) = \Phi(i, \theta) + \Psi(i) \qquad (28)$$

where

$$\Phi(i, \theta) = \int T(i, \theta) \, d\theta \qquad (29)$$

and $\Psi(i)$ is related to the part of winding inductance, which is independent of the rotor position, i.e., L_a.

By conducting torque measurements at a sufficient number of points in the *phase current-rotor displacement* plane, a 2-D surface representing the torque surface is constructed. By computing the integral in (29), $\Phi(i, \theta)$ can be obtained. Separate measurements are then conducted to identify $\Psi(i)$.

The torque produced in a BLDCM is due to the interaction of the permanent magnet with the magnetic field created by the current flow in the stator windings as well as the reluctance effect. If only one phase (line-to-line) is conducting, the torque equation (8) is reduced to

$$T(i, \theta) = nL_G \sin(2n\theta - 2\phi)i^2 + nK_E \cos(n\theta - \phi)i \qquad (30)$$

where $L_G = 3L_g$, and $K_E = \sqrt{3} K_e$. When the saturation effect is taken into account, the parameters K_E and L_G cannot be assumed constant, and as a result, (30) does not accurately describe the behavior of the system. However, since a piecewise linear model is considered to characterize the saturation effect, it is assumed that the sinusoidal distribution of the phase windings does not change with the current variations. In other words, we will assume that the functional dependence of the torque on the rotor displacement is preserved, and only the amplitudes of the two sinusoids in (30) vary as functions of current. The torque expression for the case when magnetic saturation is present may then be written as

$$T(i, \theta) = \alpha(i) \cos(n\theta - \phi)i + \beta(i) \sin(2n\theta - 2\phi)i^2 \qquad (31)$$

where

$$\alpha(i) = nK_E(i) \qquad (32)$$

$$\beta(i) = nL_G(i). \qquad (33)$$

A. Torque Measurement: Identification of $\Phi(i, \theta)$

An experimental procedure has been designed to identify the parameters describing the characteristics associated with each line-to-line phase winding. In the experiments, one leg of the Y-connected stator phase windings is removed, and the two remaining legs carry the same amount of current at all times. The rotor is locked at a fixed position when a prescribed current is supplied to the windings; see Fig. 7. As the current rises and falls, so does the torque generated by the motor. During these variations, torque and current measure-
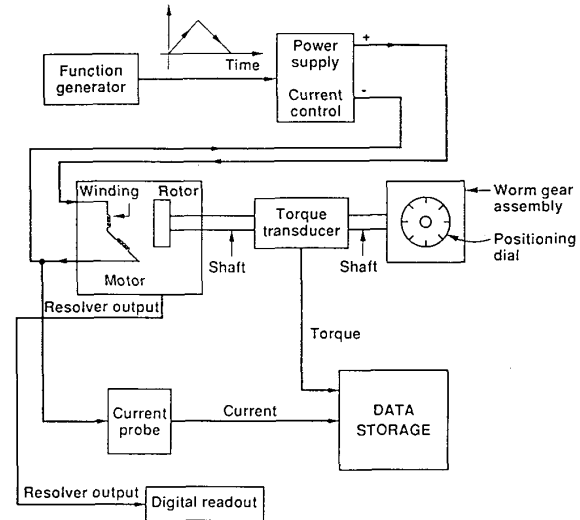

Fig. 7. Experimental setup for torque and current measurements.

ments are taken at discrete points of time. The same procedure is repeated for several rotor positions. Finally, a set of measured torques at discrete points in the $(i - \theta)$ plane are collected. Since the identification process is based on torque measurements, the frequency of the current input is kept low.

Figs. 8 and 9 show the sample data collected at different rotor positions and different current values. The curves in the figures define various cross sections of the torque surface. Keeping θ constant corresponds to the curve generated by intersecting a plane parallel to the $(T - i)$ plane with the torque surface, whereas keeping i constant corresponds to the curve generated by intersecting a plane parallel to the $(T - \theta)$ plane with the torque surface. By experimentally determining sets of such curves, the torque surface is constructed. Notice that the curves in Figs. 8 and 9 show the presence and the degree of hysteresis in the magnetic structure. The presence of the hysteresis is due to the fact that the current supplied to the windings follows a cycle of triangular signal with a peak value.

B. Inductance Measurement: Identification of $\Psi(i)$

The term $\Psi(i)$ in the coenergy function (28) depends only on current and cannot be determined by torque measurements alone. In the case of a linear magnetic structure, this term appears in the flux linkage formulation as the inductance term that is independent of rotor displacement, i.e.
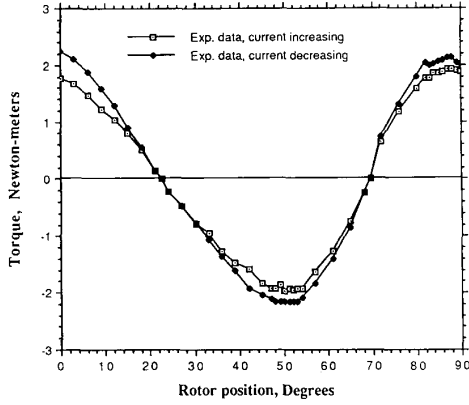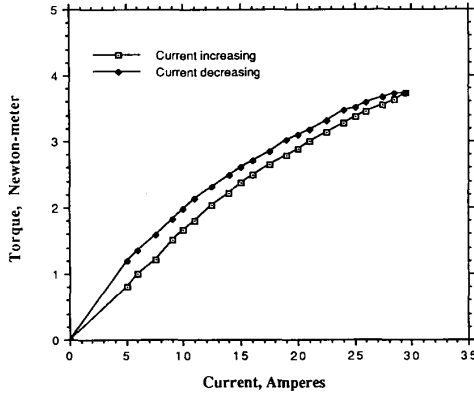
$$\Psi(i) = \frac{1}{2} L_A i^2. \qquad (34)$$

The inductance parameters L_A and L_G may be written in the following way [4], [9]:

$$L_A = K_A \mu \qquad (35)$$

$$L_G = K_G \mu \qquad (36)$$

where K_A and K_G are constant parameters that are solely functions of the geometry of the rotor and the windings, and μ is the permeability factor. Since a piecewise linear model

Fig. 8.   Experimental torque measurements at $i = 7.5$ A.

Fig. 9.   Experimental torque measurements at $\theta = 9.0°$.

has been considered for the case of magnetic saturation, one can write

$$\frac{L_A(i)}{L_G(i)} = \text{constant} . \qquad (37)$$

Since $L_G(i)$ has already been determined as a result of identifying $\Phi(i, \theta)$, it is sufficient to determine the value of L_A in the linear range of operation and then use (37) to evaluate $L_A(i)$. To identify the value of L_A in the linear range, an inductance analyzer is used to directly measure the inductance of the windings. This is done by conducting the measurements for different rotor displacements. By gathering a sufficient number of inductance measurements for a full mechanical cycle and computing the average value of the measurements, the value of L_A in the linear range is obtained.

VI. EXPERIMENTAL RESULTS

The torque data at discrete values of rotor displacements and phase currents are fitted to an analytical torque surface of the form given in (31), where $\alpha(i)$ and $\beta(i)$ are considered to be piecewise polynomials of current i. For the BLDCM studied here, three polynomials are used to represent $\alpha(i)$ and $\beta(i)$ for three separate intervals of current. The parameters defining the polynomials are computed by finding the
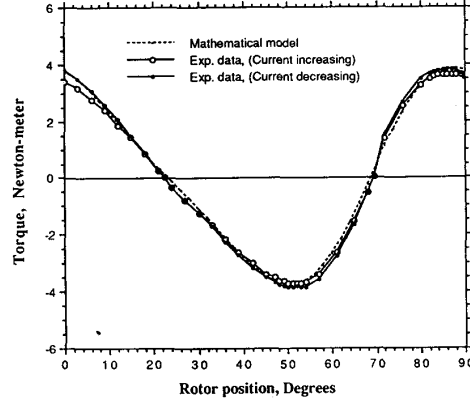
Fig. 10.   Experimental and computed torque values at $i = 15.0$ A.

best torque surface defined by (31) to the torque data in the least square error sense. The piecewise polynomial functions are required to be continuous and to have continuous first derivatives since

$$\lambda(i, \theta) = \frac{\partial \left[\int T(i, \theta) \, d\theta + \Psi(i) \right]}{\partial i} \qquad (38)$$

which implies that the torque expression must be continuous and have a continuous first derivative with respect to the variable i.

The torque surface fitting problem may be formulated as a least squares problem as follows

$$\min \| T(i, \theta) - T_d(i, \theta) \|_F \qquad (39)$$

where T_d is the matrix containing the torque data, and F denotes the Frobenius matrix norm. The expression defining the torque surface (see (29)) may be written in the following form:

$$T(i, \theta) = T_1(i, \theta) + T_2(i, \theta) \qquad (40)$$

where

$$T_1(i, \theta) = \alpha(i) \cos(n\theta) i$$
$$= (\alpha_0 + \alpha_1 i + \alpha_2 i^2 + \ldots) \cos(n\theta) i \qquad (41)$$
$$T_2(i, \theta) = \beta(i) \sin(2n\theta) i^2$$
$$= (\beta_0 + \beta_1 i + \beta_2 i^2 + \ldots) \sin(2n\theta) i^2. \qquad (42)$$

Figs. 10 through 13 show the resultant approximating functions fitted to the experimental data at various values of θ and i. To see the overall behavior of the torque generated by one phase winding as a function of rotor position and phase current, Fig. 14 depicts the torque surface generated by the mathematical model. To further examine the accuracy of the mathematical model, a set of independent experimental data are used.[1] Fig. 15 depicts the predicted values of the line-to-line phase winding inductance as a function of rotor displace-

---

[1] The set of independent experimental data correspond to tests performed on a motor unit with the same manufacturer serial number, i.e. MOOG 303-003, as the one used in the modeling procedure presented here. The data were provided by the engineers at MOOG.
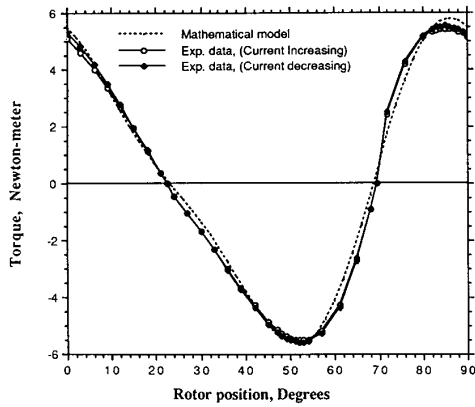
Fig. 11.   Experimental and computed torque values at $i = 25.0$ A.
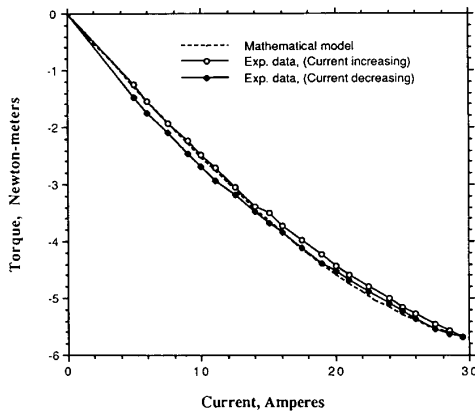
Fig. 12.   Experimental and computed torque values at $\theta = 47.0°$.
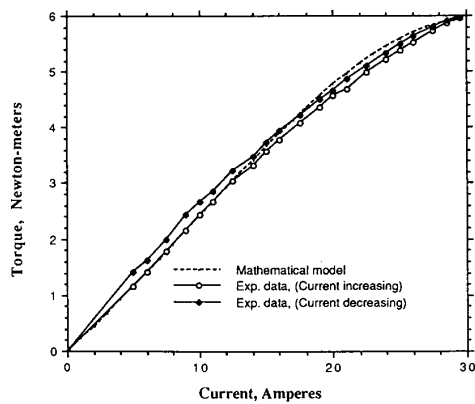
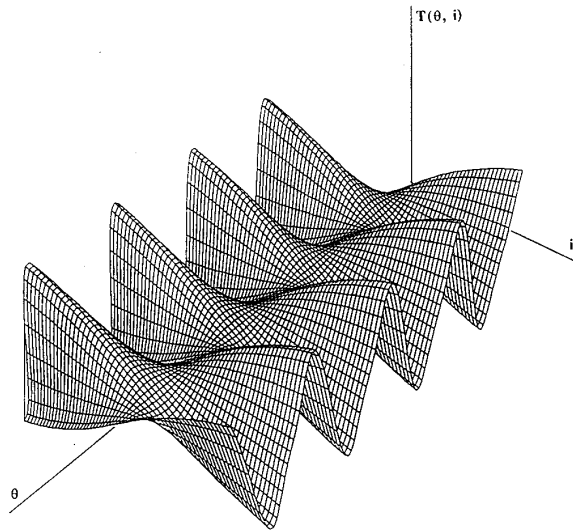Fig. 13.   Experimental and computed torque values at $\theta = 83.0°$.

Fig. 14.   Torque surface for a line-to-line phase winding based on the mathematical model.
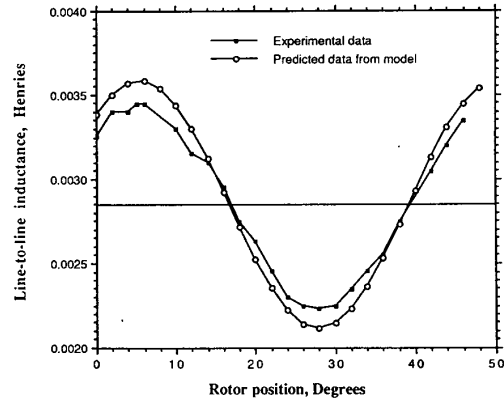

Fig. 15.   Experimental and computed values of the phase winding inductance (line to line).
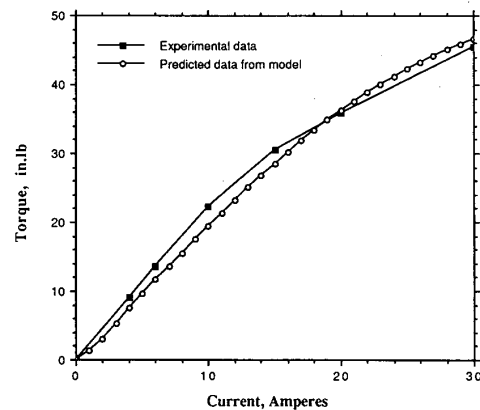
Fig. 16.   Experimental and computed torque versus current curves at $\omega = 200$ r/min.

ment compared with the experimental data. Fig. 16 shows the torque-current data of the BLDCM at a constant rotor speed. The agreement between the predicted values and the experimental data are quite good, especially considering that this set of experimental data is taken from a different motor unit

than the one used for the construction of the mathematical model.

VII. CONCLUSIONS

An analytical and experimental study of brushless dc motors has been presented. A method for constructing a BLDCM model, which accounts for magnetic saturation and reluctance variation effects, has been presented. Based on a piecewise linear magnetic structure, an experimental procedure has been outlined and implemented to identify the parameters describing the characteristics of a BLDCM. Using the experimental data obtained from torque and phase current measurements, a mathematical model of the 2-D torque surface was obtained by solving the corresponding least squares problem. The accuracy of the resulting mathematical model was successfully checked against independent experimental measurements.

ACKNOWLEDGMENT

REFERENCES

[1] H. Asada and K. Youcef-Toumi, *Direct Drive Robots: Theory and Practice.* Cambridge, MA: MIT Press, 1987.
[2] H. D. Chai, "Permeance model and reluctance force between toothed structures," in *Theory and Applications of Step Motors.* St. Paul, MN: West, 1974.
[3] N. A. Demerdash, T. W. Nehl, and E. Maslowski, "Dynamic modeling of brushless dc motors in electric propulsion and electromechanical actuation by digital techniques," in *IEEE/IAS Conf. Rec.* (Cincinnati), 1980, pp. 570–579.
[4] A. E. Fitzgerald, C. Kingsley, and S. D. Umans, *Electric Machinery.* New York: McGraw-Hill, 1983, 4th ed.
[5] N. Hemati, "Modeling, analysis, and tracking control of brushless dc motors for robotic applications," Ph.D. thesis, Sibley School Mech. Aerospace Eng., Cornell Univ., Aug. 1988.
[6] N. Hemati and M. Leu, "Accurate modeling of brushless dc motors for high-performance applications," in *Proc. 18th Ann. Symp. Incremental Motion Contr. Syst. Devices,* June 1989, pp. 89–96.
[7] M. Ilic-Spong, R. Marino, S. M. Peresada, and D. G. Taylor, "Feedback linearizing control of switched reluctance motors," *IEEE Trans. Automat. Contr.,* vol. AC-32, no. 5, pp. 371–379, May 1987.
[8] M. Ilic-Spong, T. J. E. Miller, S. R. MacMinn, and J. S. Thorp, "Instantaneous torque control of electric motor devices," *IEEE Trans. Power Electron.,* vol. PE-2, no. 1, pp. 55–61, Jan. 1987.
[9] T. M. Jahns, "Torque production in permanent-magnet synchronous motor drives with rectangular current excitation," *IEEE Tras. Industry Applications,* vol. IA-20, no. 4, pp. 803–813, July/Aug. 1984.
[10] P. C. Krause, *Analysis of Electric Machinery.* New York: McGraw-Hill, 1986.
[11] P. C. Krause, R. R. Nucera, R. J. Krefta, and O. Wacynczuk, "Analysis of a permanent magnet synchronous machine supplied from a 180° inverter with phase control," *IEEE Trans. on Energy Conversion,* vol. EC-2, no. 3, pp. 423–431, Sept. 1987.
[12] C. L. Lawson and R. J. Hanson, *Solving Least Squares Problems.* Englewood Cliffs, NJ: Prentice-Hall, 1974.
[13] D. G. Manzer and M. Verghese, "Robot motor modelling revisited: A complete 3-D characterization," IBM Tech. Rep., July 1987.
[14] S. Meshkat, "A new microprocessor based brushless servo amplifier for optimum current vector control," in *Proc. 13th IMCSD Ann. Symp.,* 1984, pp. 19–24.
[15] P. Muir and C. Neuman, "Pulsewidth modulation control of brushless dc motors for robotic applications," *IEEE Trans. Ind. Electron.,* vol. IE-32, no. 3, pp. 222–229, Aug. 1985.
[16] S. Murugesan, "An overview of electric motors for space applications," *IEEE Trans. Ind. Elect. Contr. Instrum.,* vol. IECI-28, no. 4, Nov. 1981.
[17] E. K. Persson and M. Buric, "Mathematical modelling and simulation of high performance brushless dc motors," in *Proc. IMCSD 5th Ann. Symp.,* 1976, pp. W1–W8.
[18] G. Pfaff, A. Weschta, and A. Wick, "Design and experimental results of a brushless ac servo-drive," *IEEE Trans. Industry Applications,* vol. IA-20, no. 4, pp. 814–821, July/Aug. 1984.
[19] W. F. Ray *et al.,* "High performance switched reluctance brushless drives," in *Proc. IEEE/IAS,* 1985, pp. 1769–1776.
[20] J. Tal, "Optimal commutation of brushless motors," in *Proc. IMCSD 11th Ann. Mtg.,* 1982, pp. 49–53.
[21] M. Vidyasagar, "System theory and robotics," *IEEE Contr. Syst. Mag.,* pp. 16–17, Apr. 1987.
[22] D. C. Youla and J. J. Bongiorno, Jr., "A floquet theory of the general rotating machine," *IEEE Trans. Circuits Syst.,* vol. CAS-27, no. 1, pp. 15–19, Jan. 1980.

Neyram Hemati (M'88) was born in Tehran, Iran, on August 18, 1960. He received the Ph.D. and the Master of Engineering degrees in August 1988 and January 1984, respectively, from the Sibley School of Mechanical and Aerospace Engineering at Cornell University, Ithaca, NY, and the Bachelor of Science degree in mechanical engineering from Iowa State University, Ames, in December 1982.

In September 1988, he joined the faculty of Drexel University, Philadelphia, PA, where he is currently an Assistant Professor in the Department of Mechanical Engineering and Mechanics. His research interests include modeling and control of electromechanical systems, computer and microprocessor control, applied nonlinear control, and robotics.

Dr. Hemati is a member of ASME, IEEE, Pi-Tau-Sigma, and Sigma-Xi.
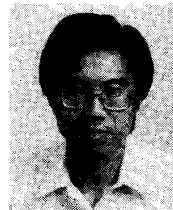
Ming C. Leu (M'89) received the Ph.D. degree in 1981 from the University of California at Berkeley, the M.S. degree in 1977 from Pennsylvania State University, State College, and the B.S. degree in 1972 from the National Taiwan University, all in mechanical engineering.

He is currently Professor of Mechanical Engineering and holder of the New Jersey Chair in Manufacturing/Productivity at the New Jersey Institute of Technology, Newark. From 1981 to 1987, he was a faculty member at the Sibley School of Mechanical and Aerospace Engineering, Cornell University, Ithaca, NY. His research interests include electromechanical systems, dynamics and control, robotics, and CAD/CAM. He has authored over 70 refereed technical publications.

Dr. Leu received a Presidential Young Investigator Award (1985), a Ralph R. Teetor Educational Award (1985), and a Wood Award (1981). He is a member of Sigma Xi, Tau Beta Pi, and Phi Kappa Phi. Professionally, he is a member of ASME, IEEE, SME, and CIRP. He served as an Executive Committee Member, including chairmanship, of ASME Production Engineering Division from 1986-1990. He has served on the Organizing and Program Committees of U.S.A.-Japan Symposium on Flexible Automation in 1986, 1988, 1990, and is the 1992 Program Chairman for this Symposium. He has organized and edited the proceedings of six manufacturing related conferences. He is a member of the Editorial Board of Journal of Systems Integration.